2025, 10(44s) e-ISSN: 2468-4376

https://www.jisem-journal.com/

Research Article

Estimating Solar Energy Potential in the High-Altitude Region of Jumla, Nepal, using RadEst 3.0 ver. Software

Binod Kharel ¹, Anil Thapa ², Kishor Khatiwada ³, Sourav Rijal ⁴, Basanta Kumar Rajbanshi ⁵, Khem Narayan Poudyal ⁶

¹ Research Scholar, Patan Multiple Campus, Tribhuvan University, Kathmandu, Nepal. Email: binodkharel2046@gmail.com
 ² Research Scholar, St. Xavier's College, Tribhuvan University, Kathmandu, Nepal. Email: cherthapa@gmail.com
 ³ Research Scholar, St. Xavier's College, Tribhuvan University, Kathmandu, Nepal. Email: kishorkhatiwadasxc@gmail.com
 ⁴ Research Scholar, Patan Multiple Campus, Tribhuvan University, Kathmandu, Nepal. Email: saurabrijal35@gmail.com

5 Research Scholar, Shri Ramswaroop Memorial University, Devaroad-Lucknow, Barabanki, India. Email: basantaraz22@gmail.com_ORCID ID: 0009-0003-7953-7475

⁶ Professor, Pulchowk Campus Institute of Engineering, Tribhuvan University, Kathmandu, Nepal. Email: khem@ioe.edu.np

ARTICLE INFO

ABSTRACT

Received: 20 Dec 2024

Revised: 19 Feb 2025

Accepted: 28 Feb 2025

Solar energy, a clean, renewable, and sustainable resource, has become a key energy alternative in the 21st century. Despite its global availability, over 70% of Nepal's energy still comes from conventional sources, emphasizing the need for solar energy assessments. Situated within the global solar energy belt, Nepal has significant potential for solar power utilization.

This study evaluates solar energy potential in Jumla (29.28°N, 82.16°E, 2300 m altitude), a midwestern mountainous region of Nepal. Meteorological parameters were processed using RadEst 3.0 software, which applied auto-optimization and parameter-fitting techniques to estimate solar radiation. Predicted values were validated against observed data using four empirical models: Bristow and Campbell (BC), Campbell and Donatelli, Donatelli and Bellocchi, and the Modular DCBB model.

The BC model demonstrated the best performance, yielding higher radiation estimates with lower mean bias error (MBE), root mean square error (RMSE), and coefficient of residual mass (CRM). The annual average solar energy was 18.9 $\rm MJ/m^2/day$ in 2021, 19.3 $\rm MJ/m^2/day$ in 2022, and 19.6 $\rm MJ/m^2/day$ in 2023, with RMSE values of 3.76, 3.81, and 3.99 $\rm MJ/m^2$, respectively. These results confirm the BC model's reliability and its applicability for solar energy prediction in similar regions of Nepal.

Keywords: Meteorological parameters, RadEst 3.00 software, model coefficients, solar energy, statistical tools.

INTRODUCTION

Nepal, located at an average latitude of 27.5°N, lies close to the global solar belt (15°-35° latitude) (Acra et al., 1984). The country receives substantial solar energy, ranging between 12.93 and 22.48 megajoules per square meter per day, with approximately 300 sunny days annually. (J. R. Shrestha, 1998). Various studies have confirmed that Nepal's average solar energy potential falls between 3.6 and 6.2 kWh/m²/day (J. Shrestha et al., 2003) (Pondyal et al., 2011).

Jumla, located in Karnali Province, spans roughly 2,531 km² and is situated at 29.28°N latitude and 82.16°E longitude, with an elevation of 2,300 meters above sea level (P. M. Shrestha et al., 2019). Due to its proximity to the solar belt, the region experiences considerable temperature fluctuations, with summer temperatures varying between 12° C and 30° C, and winter temperatures ranging from -11° C to 12° C. Jumla receives an estimated 18.28 MJ/m²/day of solar energy annually, surpassing the levels found in Nepal's hill and Terai regions. Additionally, the area records one of the lowest annual precipitation levels in the country, around 900 mm (Khatri Chhetri & Gurung, 2017).

2025, 10(44s) e-ISSN: 2468-4376

https://www.jisem-journal.com/

Research Article

(Rajbanshi et al., 2025) applied RadEst 3.0 software to estimate GSR in the eastern upland area of Taplejung, Nepal. Similarly, (Rajbanshi et al., 2024A) used the same software to calculate daily GSR in Dhankuta, a hilly region in eastern Nepal. Both studies highlight the variation in solar energy across Nepal's diverse topography and provide valuable insights for optimizing solar energy utilization in different regions. Additionally, (Joshi et al., 2022) employed RadEst 3.0 to determine daily GSR in Simikot, a high-altitude location in western Nepal, further demonstrating the software's applicability in diverse terrains.

In another study, (Rajbanshi et al., 2024B) employed RadEst 3.0 to determine daily GSR in Biratnagar, a lowland city in eastern Nepal. The findings indicate significant differences in solar energy potential between lowland and highland regions, influenced by altitude, atmospheric conditions, and cloud cover. The higher solar energy levels observed in mountainous areas, compared to the Terai, are primarily attributed to reduced atmospheric pollution and lower cloud cover at higher altitudes (Poudyal et al., 2012).

These studies collectively emphasize Nepal's potential for harnessing solar energy and highlight the need for region-specific solar energy policies and infrastructure development.

Energy plays a crucial role in various sectors, including agriculture, households, transportation, industry, commerce, and education. It is a key indicator of quality of life globally (Joshi et al., 2022). Furthermore, energy consumption is directly linked to socioeconomic activities and overall national development. Approximately 83% of Nepal's citizens live outside urban centers, highlighting the importance of implementing sustainable energy solutions (Poudyal, 2015).

Currently, approximately 70% of Nepal's total energy consumption comes from traditional sources such as fuelwood, agricultural waste, and animal excreta, mainly utilized for heating and meal preparation in non-urban and semi-urban regions. This dependence on conventional energy stems from the scarcity of renewable and modern energy alternatives for household lighting, food preparation, and other domestic needs. The country's total energy consumption is composed of 68.7% conventional energy, 28.1% commercial energy, and only 3.2% renewable energy (Economic Survey 2019/20) (Government of Nepal, 2020). Additionally, Nepal lacks its own fossil fuel resources and is landlocked, with hydropower accounting for less than 5% of the nation's total energy consumption (WECS, 2023).

Mapping the spatial distribution of solar irradiance over a large region would require several hundred ground stations (Schillings et al., 2004). However, in developing countries like Nepal, establishing such an extensive network of ground-based measurements is not feasible due to financial and technical constraints. To overcome this limitation, several models and software tools, including RadEst 3.0, have been designed to calculate solar energy using meteorological data derived from climatic variables (Donatelli & Bellocchi, 2001a).

In this study, we utilize RadEst 3.0 software to evaluate different empirical models for estimating solar energy. The models utilize meteorological data, such as daily high and low temperatures along with rainfall measurements, to identify the most effective method for accurately estimating solar radiation levels in Nepal.

MODELS

RadEst 3.0 is an application compatible with MS Windows platforms (98/NT/2000/XP), developed to assist in estimating solar energy values using a specified latitude. The software incorporates four fundamental models—Bristow-Campbell, Campbell-Donatelli, Donatelli-Bellocchi, and the Modular Donatelli-Campbell-Bristow-Bellocchi (MDCBB) model (Chegaar et al., 1998) (Joshi et al., 2021). These models analyze results using both graphical and statistical tools, employing specific parameters to assess solar energy estimates effectively.

 tt_i = transmissivity,

 τ = clear sky transmissivity,

 ΔT = average monthly temperature (°C),

 T_{max} = daily maximum air temperature (°C),

2025, 10(44s) e-ISSN: 2468-4376

https://www.jisem-journal.com/

Research Article

 T_{min} = daily minimum air temperature (°C),

b = coefficient of temperature range. The parameter b serves as a crucial component across all models,

c = highly sensitive empirical factor, meaning even minor variations in its value can lead to significant changes in the estimated solar energy output.

 T_{nc} = empirical factor representing the summer nighttime temperature influence.

 c_1 = coefficient indicating the intensity of seasonal variation,

 c_2 = pattern or shape of that seasonal variation,

i = day of the year, i = 1 to 365,

 $f(T_{avg})$ = function dependent on the mean daily temperature,

 $f(T_{min})$ = function based on the minimum daily temperature,

 $EstRad_i$ = estimated solar energy (in MJ m⁻² day⁻¹)

 $PotRad_i$ = possible solar energy available beyond the Earth's atmosphere (in MJ m⁻² day⁻¹)

Each of the four models calculates atmospheric transmissivity for solar energy by considering the variation in air temperature between the daily maximum and minimum. The estimated solar energy value (EstRadi) is determined by multiplying the estimated transmissivity (tti) by the potential solar energy available outside Earth's atmosphere.

$$EstRad_{i} = tt_{i} \times PotRad_{i} \tag{1}$$

The potential solar energy is estimated as

$$PotRaddoy = \frac{\{117.5 \ dd2 \ hs \ Sin(lat) \ Sin(dec) + Cos(lat) \ Cos(dec) \ Sin(hs)\}}{\pi}$$

Where,

 $PotRad_{doy}$ = Potential Energy

doy = day of the year

dd2 = factor used to determine the sun's distance

 $= 1 + 0.0334 \times \cos(0.01721 \times doy - 0.0552)$

 h_s = half day length = Cos⁻¹{-Tan(dec) × Tan(lat)}

lat = latitude of the monitoring site

dec = Sun's angular position

 $= \sin^{-1}[0.39785 \times \sin \{4.869 + 0.0172 \times doy + 0.03345 \times \sin (6.224 + 0.0172 \times doy)\}]$

A brief overview of the four models in RadEst 3.00 software is provided below.

2025, 10(44s) e-ISSN: 2468-4376

https://www.jisem-journal.com/

Research Article

Bristow and Campbell Model (Bristow & Campbell, 1984)

The Bristow and Campbell (BC, 1984) model is the foundational model in RadEst 3.0, serving as the basis for the development of other models. It estimates the daily influx of solar energy by analyzing how variations in daytime and nighttime temperatures correspond to energy demand. (Iqbal, 1983). Over the years, this model has been widely applied in various studies, with continuous improvements enhancing its accuracy and applicability.

Estimated transmissivity is

$$tt_i = \tau \left[1 - \exp\left(\frac{-b\Delta T_i^c}{month\Delta T}\right) \right] \tag{2}$$

Thus,

$$EstRad_{i} = \tau \left[1 - \exp\left(\frac{-b\Delta T_{i}^{c}}{month\Delta T}\right) \right] \times PotRad_{i}$$
(3)

Where,

$$\Delta T = T_{max_i} - \frac{(T_{min_i} + T_{min_{i+1}})}{2}$$

Campbell and Donatelli Model (M Donatelli & GS, 1998)

The "Campbell and Donatelli" model, developed in 1998, is the second model derived from modifications to the BC Model for estimating solar energy. In this model (CD, 1998), a correction factor is included to account for seasonal variations in mid-latitude regions like Nepal. The transmissivity estimate is adjusted by a factor Tnc, which represents the temperature adjustment factor for nighttime conditions during the summer (Bechini et al., 2000).

The estimated transmissivity is

$$tt_i = \tau \left[1 - \exp\left\{ -b \times f\left(T_{avg}\right) \times \Delta T_i^2 \times f\left(T_{min}\right) \right\} \right] \tag{4}$$

Thus.

$$EstRad_{i} = \tau \left[1 - \exp\left\{-b \times f\left(T_{ava}\right) \times \Delta T_{i}^{2} \times f\left(T_{min}\right)\right\}\right] \times PotRad_{i}$$
(5)

Where

$$\Delta T = T_{max_i} - \frac{(T_{min_i} + T_{min_{i+1}})}{2}$$

$$f(T_{ava}) = 0.017 \exp f \exp(-0.053 - T_{ava})$$

$$T_{avg} = \frac{(T_{max_i} + T_{min_i})}{2}$$

$$f(T_{min}) = \exp\left(\frac{T_{min_i}}{T_{nc}}\right)$$

Donatelli and Bellocchi Model (Donatelli & Bellocchi, 2001b)

The third model in RadEst 3.00 is the Donatelli and Bellochi Model (DB, 2001), designed to estimate solar energy using air temperature data. Unlike the previous models, this one (DB, 2001) improves upon them by explicitly accounting for seasonal variations in atmospheric clarity and temperature range, modelled through a trigonometric function defined by parameters c_1 and c_2 .

2025, 10(44s) e-ISSN: 2468-4376

https://www.jisem-journal.com/

Research Article

The estimated transmissivity is

$$tt_i = \tau[1 + f(i)] \left[1 - \exp\left\{ \frac{-b\Delta T_i^2}{\Delta T_{week}} \right\} \right]$$
 (6)

Thus,

$$EatRad_{i} = \tau[1 + f(i)] \left[1 - exp \left\{ \frac{-b\Delta T_{i}^{2}}{\Delta T_{week}} \right\} \right] \times PotRad_{i}$$
 (7)

Where,

$$\Delta T = T_{max_i} - \frac{(T_{min_i} + T_{min_{i+1}})}{2}$$

$$f(i) = c_1 \left\{ sin \left(i \times c_2 \times \frac{\pi}{180} \right) + cos \left(i \times f(c_2) \times \frac{\pi}{180} \right) \right\}$$

$$f(c_2) = 1 - 1.90 \times c_3 + 3.83 \times c_3^2$$

$$c_3 = c_2 - integer(c_2)$$

Donatelli-Campbell-Bristow-Bellocchi model (Modular DCBB Model) or (MDCBB) or (DCBB) (Donatelli et al., 2003)

The fourth model in RadEst 3.00 is the Donatelli-Campbell-Bristow-Bellocchi model (Modular DCBB Model), also known as MDCBB or DCBB. This model, based on air temperature data, is designed to estimate solar energy and incorporates features from the previous three models, with the option to enable or disable these features. Significantly, the trigonometric function representing seasonal changes in clear sky transmissivity and Delta T can be eliminated by assigning a value of 0 to the parameter c1. The DCBB model defaults back to the BC model when the Tnc component is disabled and the option for using average monthly ΔT is chosen.

The estimated transmissivity is

$$tt_i = \tau[1 + f(i)] \left[1 - \exp\left\{ \frac{-b\Delta T^2 f(T_{\min})}{\Delta T_{\text{avg}}} \right\} \right]$$
 (8)

Thus

$$EstRad_{i} = \tau[1 + f(i)] \left[1 - exp \left\{ \frac{-b\Delta T^{2} f(T_{min})}{\Delta T_{avg}} \right\} \right] \times PotRad_{i}$$
(9)

Where,

$$\Delta T = T_{max_i} - \frac{(T_{min_i} + T_{min_{i+1}})}{2}$$

$$f(i) = c_1 \left\{ \sin \left(i \times c_2 \times \frac{\pi}{180} \right) + \cos \left(i \times f(c_2) \times \frac{\pi}{180} \right) \right\}$$

$$f(c_2) = 1 - 1.90 \times c_3 + 3.83 \times c_3^2$$

$$c_3 = c_2 - integer(c_2)$$

$$f(T_{avg}) = 0.017expfexp(-0.053 - T_{avg})$$

$$T_{avg} = \frac{(T_{max_i} + T_{min_i})}{2}$$

$$f(T_{\min}) = \exp\left(\frac{T_{\min_i}}{T_{\text{nc}}}\right)$$

Instrumentation:

2025, 10(44s) e-ISSN: 2468-4376

https://www.jisem-journal.com/

Research Article

To estimate solar energy, a pyranometer must be installed. Environmental data for Jumla were collected using the CMP-6 Pyranometer, which was placed in Jumla (Latitude 29.28°N, Longitude 82.16°E, and Altitude 2300 meters above sea level). The specifications of the CMP-6 model are as follows:

- Spectral range: 285 to 2800nm
- High sensitivity in the range of 5 to 20 $\mu/V/W/m^2$
- Maximum solar irradiance: about 2000 W/m²
- Directional response: up to 800 with 100 W/m² beam
- Sensitivity depends on temperature: for -100°C to +400°C, it remains less than 4%
- Special features: reliable in all-weather performance, easy to use, low noise, fast response time (about 18 seconds), and low power consumption.

The LOGBOX SD data logger captures measurement data at one-minute intervals continuously over a 24-hour period. This data is stored for long-term use via an SD memory card inserted into the device. For data transmission, the LOGBOX supports communication through either RS232 or RS485 ports (Kipp & Zonnen, 2006).

The four models in the RadEst 3.00 software use yearly data that includes the day of the year, daily rainfall, maximum and minimum temperatures, and solar radiation (DOY, Rain, Tmax, Tmin, Rad). This data should be in ASCII format, without headers, and arranged so that each row represents one day, including values for the day number (1 to 365), rainfall in mm, Tmax and Tmin in $^{\circ}$ C, and solar radiation in MJ/m²/day. Using weather data from Jumla, Nepal, the software estimated daily global solar radiation for the years 2021, 2022, and 2023.

Input Format:

RadEst 3.0 software needs the geographic coordinates—latitude, longitude, and elevation—of the monitoring locations. The clear sky transmissivity value must fall between 0.6 and 0.8. Each model incorporates this transmissivity to compute the atmospheric energy transmissivity coefficient. Latitude is particularly important, as it is used not only in estimating potential solar energy but also in the calculation and visualization of solar energy data.

Analysis:

This approach requires a minimum of two years of data to estimate and compare solar energy. While both auto-optimisation and parameter fitting methods can be applied, parameter fitting is preferred due to the direct relationship between the factors affecting solar energy and the parameters. Adjusting the values of various parameters is essential to achieve a better alignment between the measured and estimated solar energy. During the model analysis, values for RMSE, CRM, MBE, and R² are calculated. These metrics are crucial for validating the model's estimated and measured solar energy values.

RESULTS AND DISCUSSIONS

Using Parameter Fitting (PF), all four models of the RadEst 3.00 software were calibrated based on the 2021 data from Jumla, aiming to minimise the CRM, MBE, and RMSE as much as possible. At the same time, the Coefficient of Determination (R²) should be maximized. Ultimately, the Parameter Fitting (PF) method resulted in equal values for measured and model-estimated solar energy in 2021. The average solar energy value, both measured and estimated by the model, was 18.9 MJ/m²/day in 2021. Table 1 displays the observed and model-predicted average, maximum, and total annual solar energy values for Jumla in the year 2021. It was concluded that the BC model provided results closest to the measured values compared to the CD, DB, and DCBB models. Therefore, the BC model is considered the best for estimating solar energy at selected sites in Nepal for 2021.

Table 1 Average value, maximum value and yearly total of solar energy at Jumla in 2021

2025, 10(44s) e-ISSN: 2468-4376

https://www.jisem-journal.com/

Research Article

Models	Average values (MJ/m²/day)		Maximum value (MJ/m²/day)		Yearly total (MJ/m²/year)	
	MEA	EST	MEA	EST	MEA	EST
BC	18.9	18.9	33.1	28.8	6887	6890
CD	18.9	18.9	33.1	28.4	6887	6897
DB	18.9	18.9	33.1	27.5	6887	6900
DCBB	18.9	18.9	33.1	28.5	6887	6891

The calibrated parameters obtained from the 2021 data were used to estimate solar energy for the years 2022 and 2023. At first, the auto-optimisation method was applied to evaluate all four models, which was then followed by parameter fitting to estimate solar energy. It was found that the estimated and measured values of solar radiation were very close. The parameter fitting test results for the four models are provided in Tables 2 and 3. The average solar energy values were 19.3 $MJ/m^2/day$ in 2022 and 19.6 $MJ/m^2/day$ in 2023. These tables show that the measured and estimated values, including the average, maximum, and total yearly solar energy, were closest for the BC model compared to the others. Therefore, the BC model is considered the best for estimating solar energy at selected sites in Nepal for both 2022 and 2023.

Table 2 Average value, maximum value and yearly total of solar energy at Jumla in 2022

Models	Average values (MJ/m²/day)		Maximum value (MJ/m²/day)		Yearly total (MJ/m²/year)	
Wiodels	MEA	EST	MEA	EST	MEA	EST
ВС	19.3	19.0	30.6	28.2	7046	6936
CD	19.3	18.9	30.6	28.1	7046	6906
DB	19.3	19.0	30.6	26.6	7046	6921
DCBB	19.3	19.0	30.6	28.0	7046	6924

Table 3 Average value, maximum value and yearly total of solar energy at Jumla in 2023

Models	Average values (MJ/m²/day)		Maximum value (MJ/m²/day)		Yearly total (MJ/m²/year)	
	MEA	EST	MEA	EST	MEA	EST
BC	19.6	18.9	30.9	28.6	7143	6884
CD	19.6	18.8	30.9	28.6	7143	6866
DB	19.6	18.8	30.9	27.4	7143	6878
DCBB	19.6	18.9	30.9	28.6	7143	6883

The recorded data for 2021 are relatively lower compared to those from 2022 and 2023, primarily due to a higher number of cloudy days and increased rainfall during that year.

Error Analysis:

Table 4 shows the comparison of errors between the observed and model-predicted solar energy data for 2021. In 2021, the RMSE was lower for the BC model compared to the DB and MDCBB models. The MBE was also lower for the BC model compared to the CD and DB models. Additionally, the R² value for the BC model was higher than that of the other three models. Therefore, it is confirmed that, based on statistical analysis, the BC model is the best among the four models.

Table 4: Error Analysis for 2021

2025, 10(44s) e-ISSN: 2468-4376

https://www.jisem-journal.com/

Research Article

Models	RMSE(MJ/m ²)	MBE(MJ/m²)	CRM (Unitless)	R²(Unitless)
BC	3.76	0.60	0.00	0.63
CD	3.75	0.62	0.00	0.62
DB	3.80	0.61	0.00	0.62
MDCBB	4.50	0.46	0.00	0.48

Table 5 presents the error analysis between the measured and model-estimated solar energy values for 2022. It was found that the RMSE value was comparatively lower for the BC model than for the CD and MDCBB models. The MBE was also smaller in the BC model compared to the CD and DB models. Furthermore, the R² value for the BC model was higher than that of the other three models. Thus, it can be concluded that the BC model offered the most accurate fit compared to the other three models.

Table 5: Error Analysis for 2022

Models	RMSE(MJ/m ²)	MBE(MJ/m ²)	CRM (Unitless)	R²(Unitless)
ВС	3.81	0.51	0.02	0.58
CD	3.92	0.53	0.02	0.55
DB	3.79	0.56	0.02	0.56
MDCBB	4.36	0.41	0.02	0.47

Table 6 presents the error analysis between the measured and model-estimated solar energy values for 2023. It was found that the RMSE value was comparatively lower for the BC model than for the CD and MDCBB models. The MBE was also smaller in the BC model compared to the DB model. Additionally, the R² value for the BC model was higher than that of the CD and MDCBB models and equal to the DB model. Therefore, it is concluded that the BC model provided the best fit among the four models.

Table 6: Error Analysis for 2023

Models	RMSE(MJ/m ²)	MBE(MJ/m ²)	CRM (Unitless)	R ² (Unitless)
ВС	3.99	0.57	0.04	0.59
CD	4.15	0.53	0.04	0.56
DB	3.95	0.58	0.04	0.59
MDCBB	4.46	0.46	0.04	0.50

The model's overall performance was evaluated using statistical measures like RMSE, MBE, CRM, and R². It was ultimately determined that the BC model provides the most accurate solar energy estimates for the Jumla site.

The BC model exhibited higher values for the coefficient of determination, with values of 0.63, 0.58, and 0.59 for 2021, 2022, and 2023, respectively, as shown in Fig. 1.

2025, 10(44s) e-ISSN: 2468-4376

https://www.jisem-journal.com/

Research Article

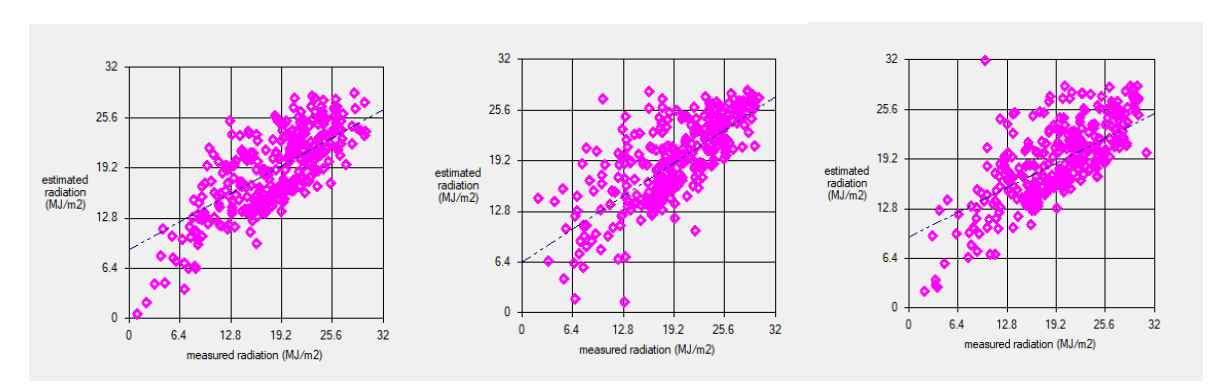


Fig. 1 The coefficient of determination in between estimated and measured value of solar energy in 2021, 2022 and 2023 of BC model

Figures 2, 3, and 4 depict the daily variation of solar energy. This variation is influenced by various factors that can affect the local weather conditions at the measurement sites, such as rainfall, humidity, and others. In Jumla, the average solar energy measured was $18.9~MJ/m^2/day$ in 2021, $19.3~MJ/m^2/day$ in 2022, and $19.6~MJ/m^2/day$ in 2023. The solid parabolic curve represents the extraterrestrial solar energy values, while the dotted scattered points indicate the measured solar energy values, which are observed in the terrestrial region.

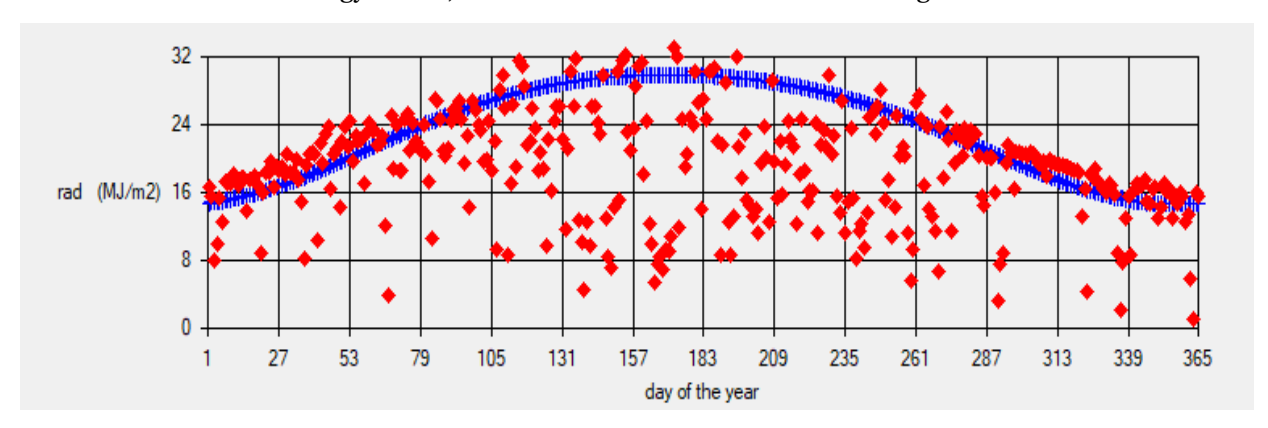


Fig. 2 Variation of Solar Energy at Jumla in 2021

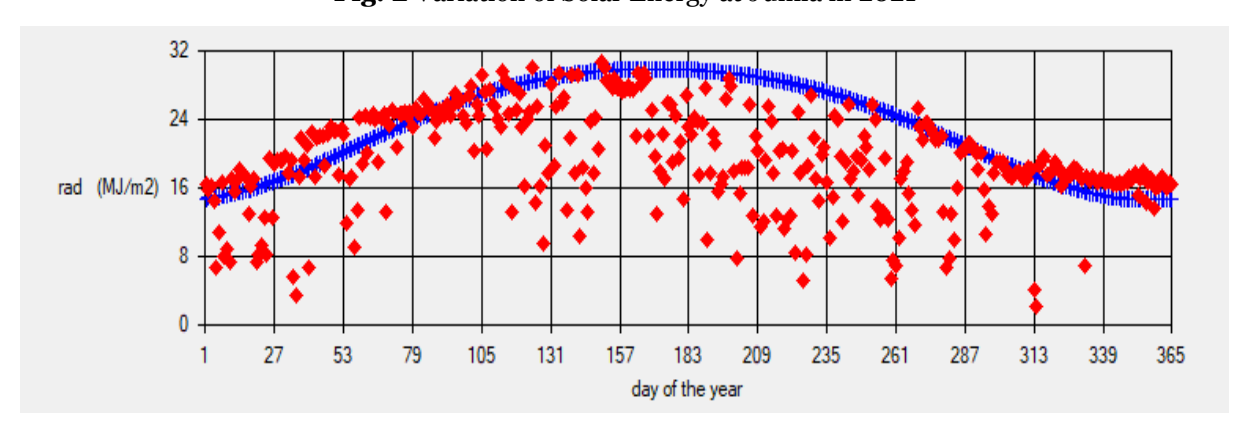


Fig. 3 Variation of Solar Energy at Jumla in 2022

2025, 10(44s) e-ISSN: 2468-4376

https://www.jisem-journal.com/

Research Article

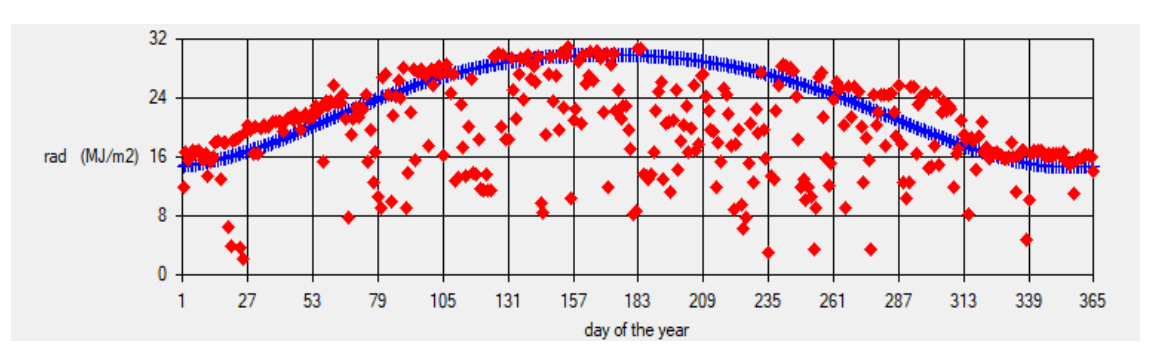


Fig. 4 Variation of Solar Energy at Jumla in 2023

Both figures show that on certain days, the measured solar radiation values exceed the extraterrestrial line. This occurs due to various physical processes, such as reflection, refraction, scattering, and diffusion, taking place in the atmosphere and on the Earth's surface.

Monthly and Seasonal variation of solar energy in 2022 and 2023

Figures 5 display the monthly and seasonal average solar energy values, both measured and estimated, for Jumla in 2022 and 2023. In 2022, the highest monthly average was 25.11 $MJ/m^2/day$ in April, and the lowest was 14.33 $MJ/m^2/day$ in January. In 2023, the highest monthly average was 24.49 $MJ/m^2/day$ in May, and the lowest was 13.30 $MJ/m^2/day$ in December. The seasonal averages in 2022 ranged from 23.40 $MJ/m^2/day$ in spring to 16.20 $MJ/m^2/day$ in winter, while in 2023, they ranged from 22.59 $MJ/m^2/day$ in spring to 16.35 $MJ/m^2/day$ in winter.

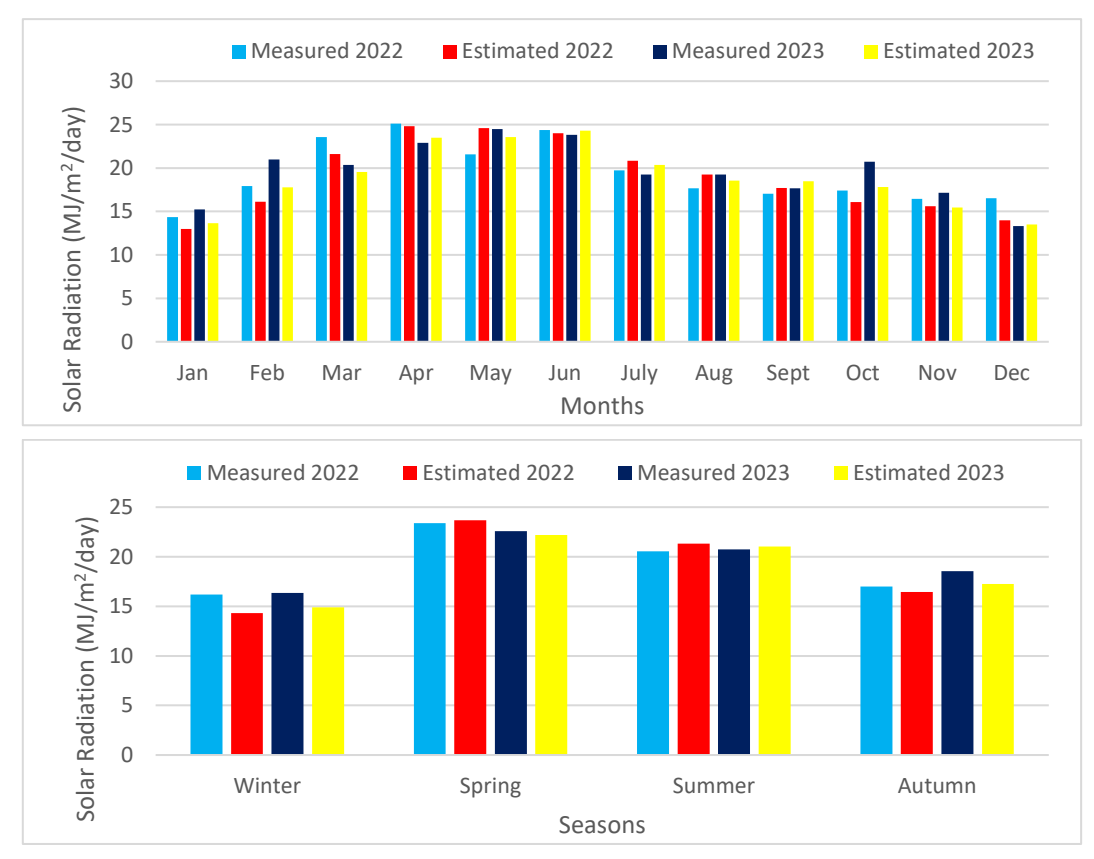


Fig. 5 Measured and Estimated value of Monthly and Seasonal variation of solar energy at Jumla in 2022 and 2023.

Ten days variation of average value of solar energy and the daily transmissivity coefficient at Jumla in 2022:

2025, 10(44s) e-ISSN: 2468-4376

https://www.jisem-journal.com/

Research Article

In Fig. 6, the measured data initially leads the estimated data, resulting in a slight overestimation of the measured values. In the middle of the year, both the measured and estimated data show fluctuations, with the measured values sometimes exceeding and at other times falling behind the estimated values. Towards the end of the year, the measured data is overestimated. This behavior is attributed to local weather conditions such as humidity, rainfall, cloud cover, and wind direction.

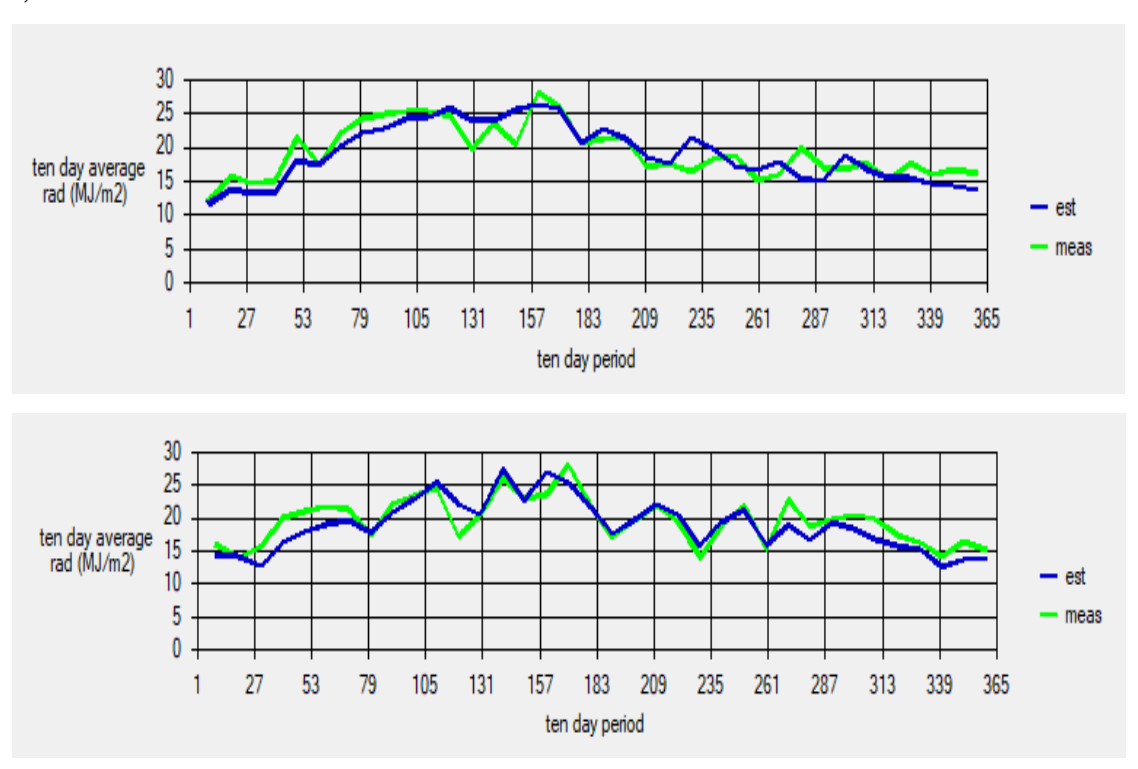
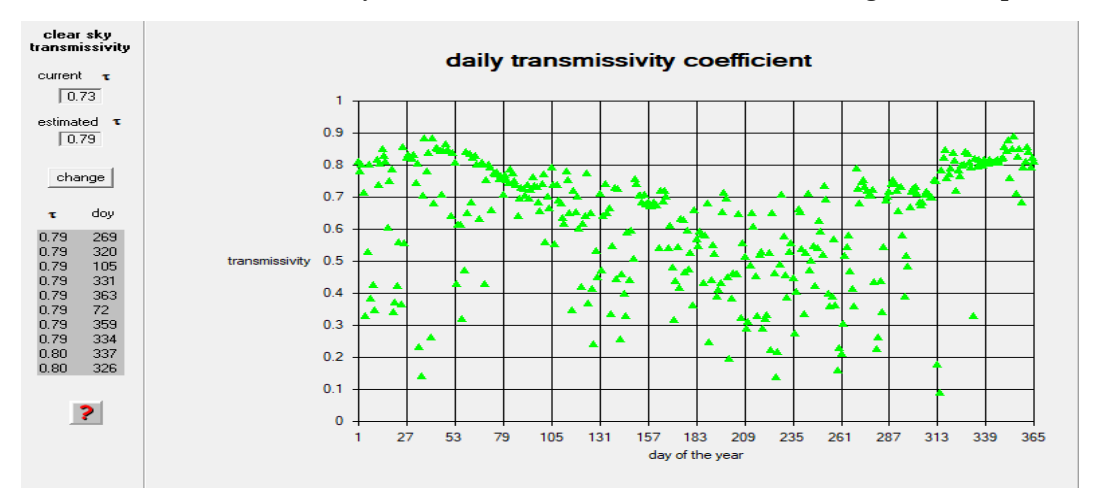


Fig. 6 Ten days variation of energy at Jumla in 2022 and 2023 shown by BC- Model with 10 days interval in a year In Fig 7, the daily transmissivity coefficient is highly fluctuated in summer season in both years due to rainfall and less fluctuated in winter season because sky is cleared in winter season at mountain region in compare to terai region.



2025, 10(44s) e-ISSN: 2468-4376

https://www.jisem-journal.com/

Research Article

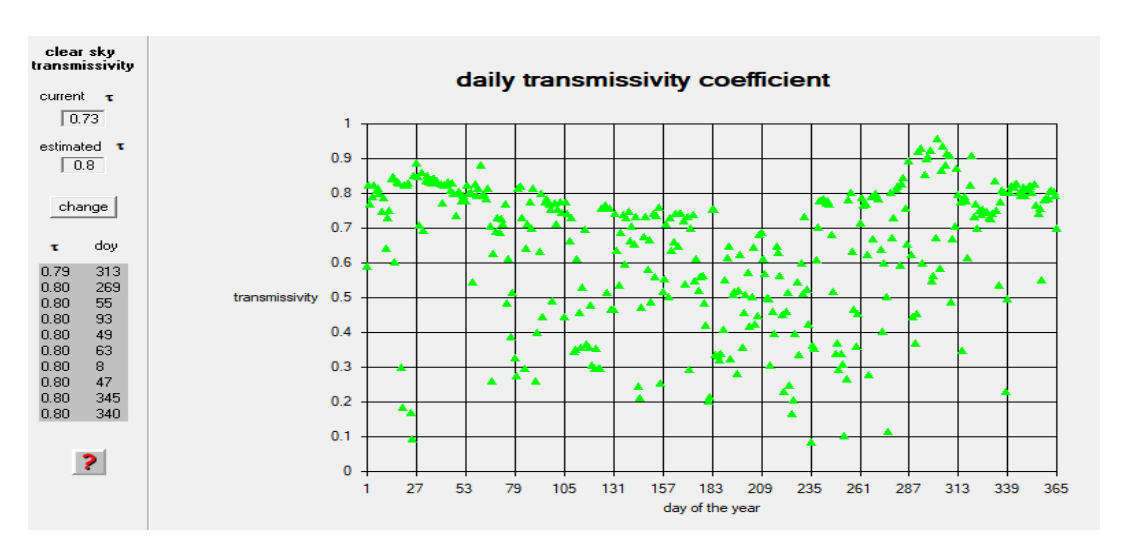
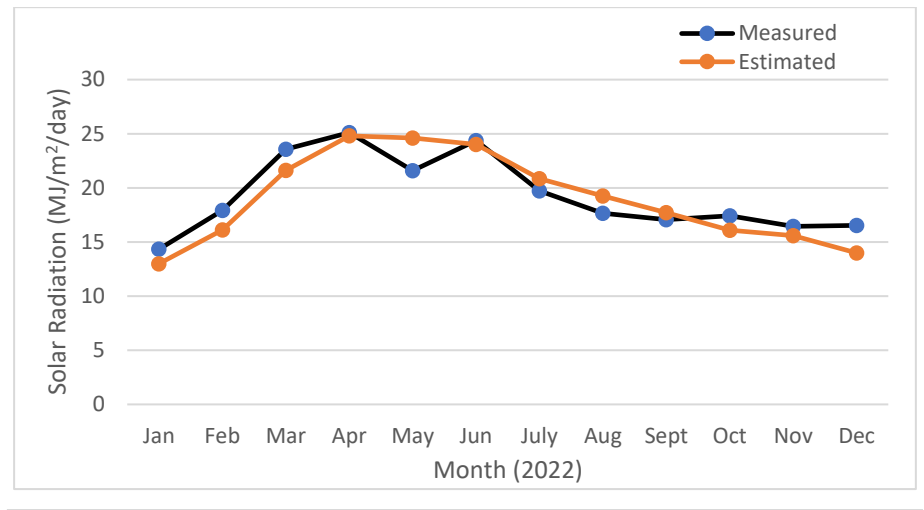
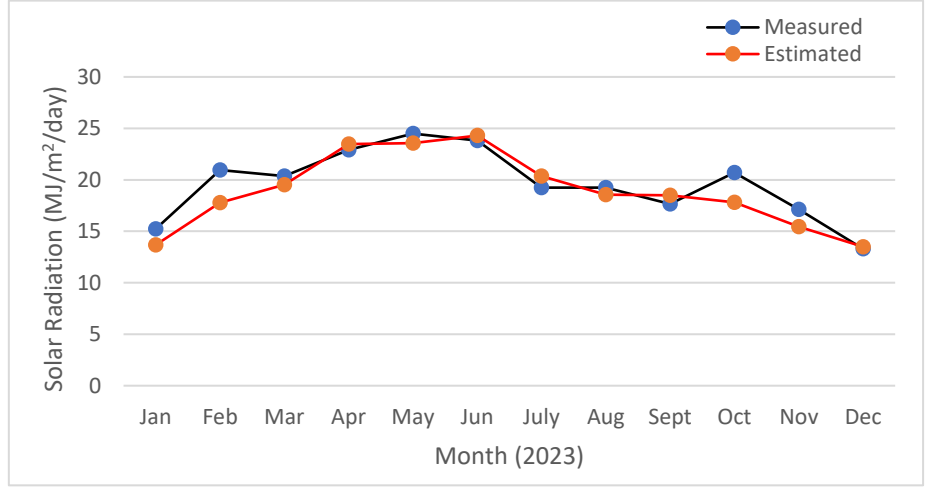


Fig. 7 Daily transmissivity coefficient at Jumla in 2022 and 2023

Graphical Representations of Variation of Estimated and Measured Solar Radiation with Month and Day of Year





2025, 10(44s) e-ISSN: 2468-4376

https://www.jisem-journal.com/

Research Article

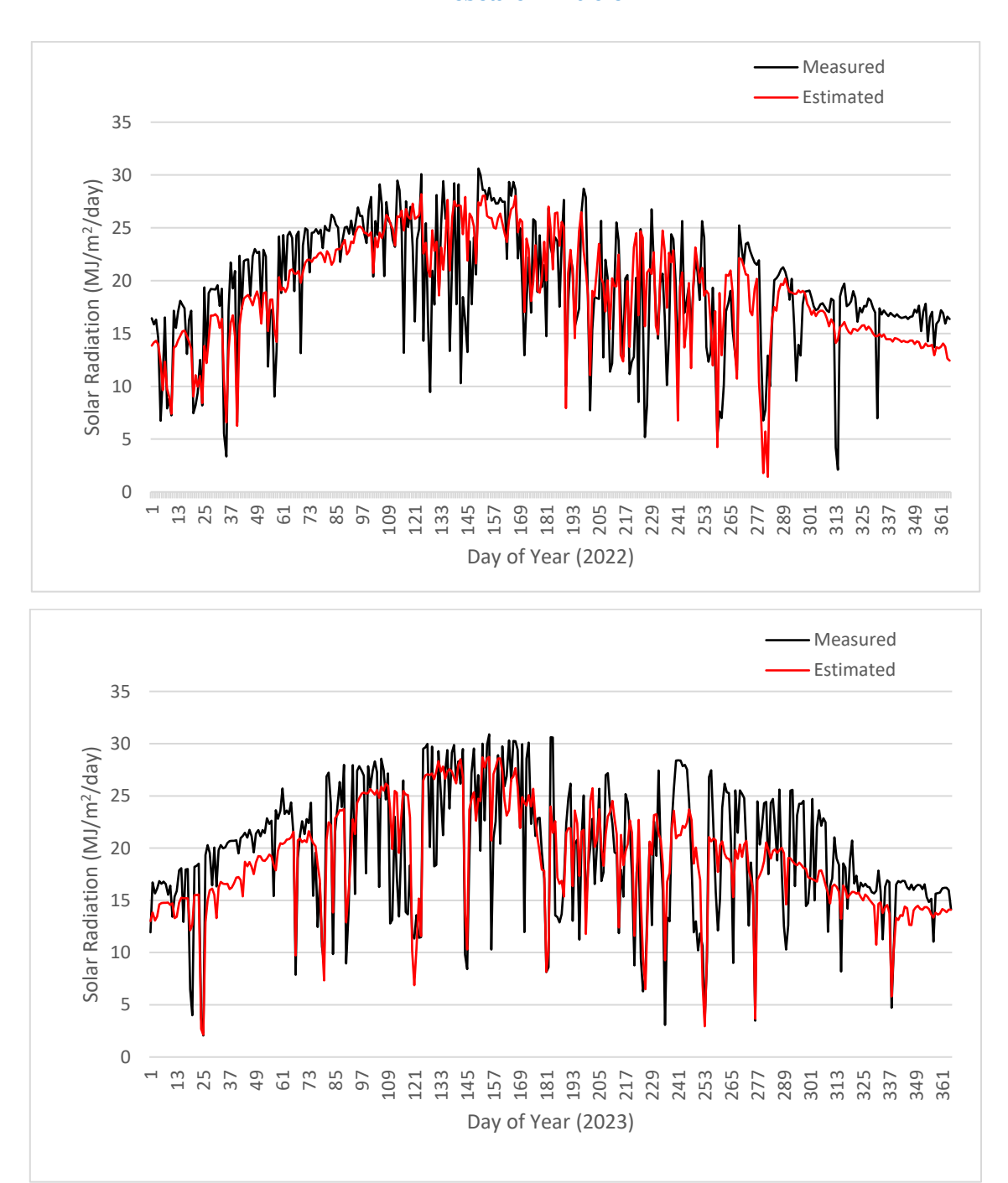


Fig. 8 Graphical Representations of Variation of Estimated and Measured Solar Radiation with Month and Day of Year 2022 and 2023 at Jumla, Nepal

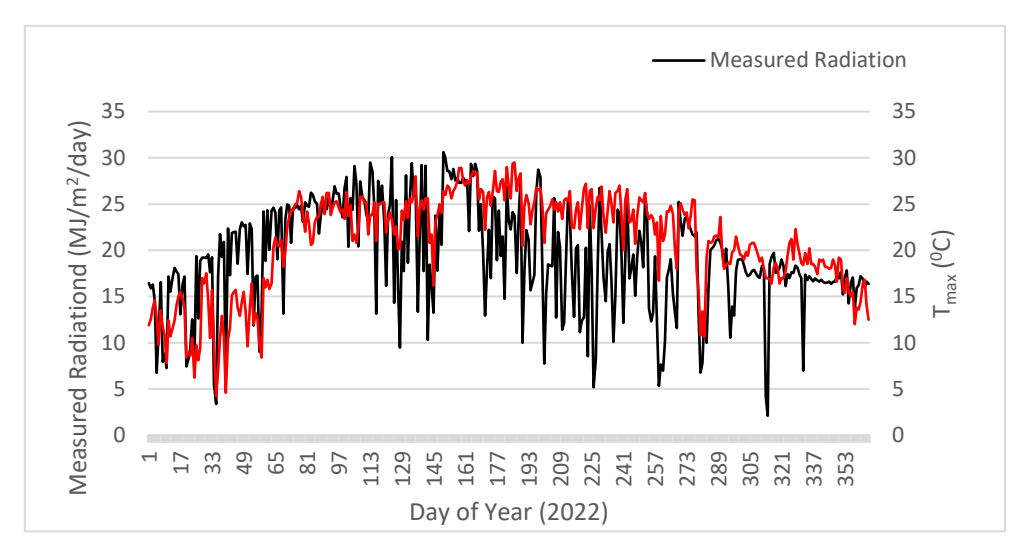
Graphical Representations of Variation Measured Solar Radiation with Temperature, Rainfall and Relative Humidity along the Day of Year

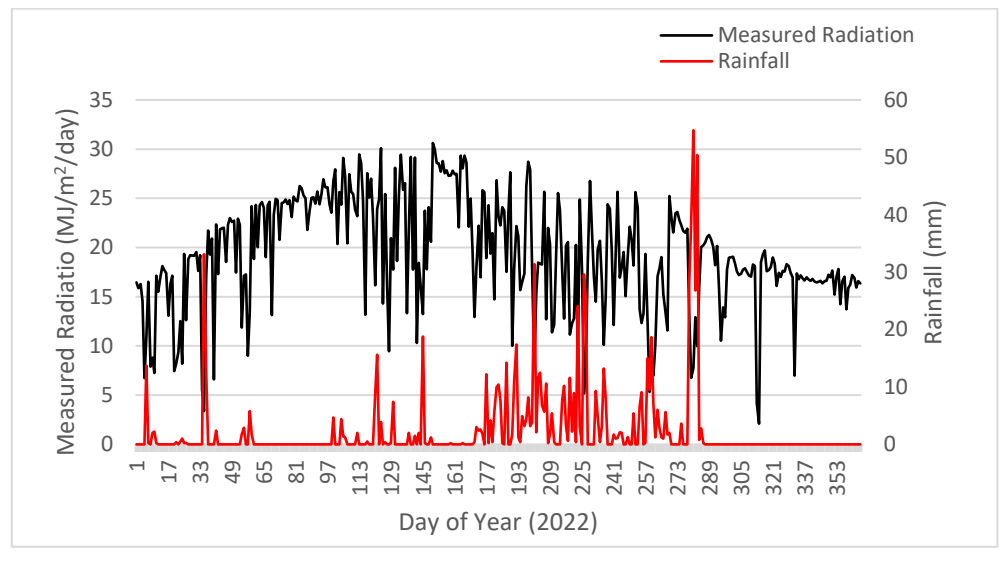
In Fig 9, measured solar radiation is directly proportional to maximum air temperature and inversely proportional to rainfall and average relative humidity.

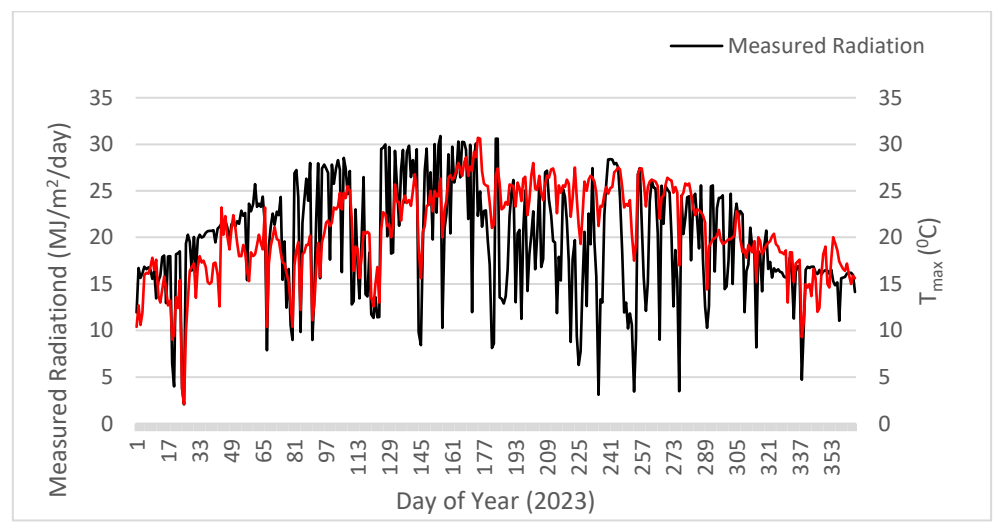
2025, 10(44s) e-ISSN: 2468-4376

https://www.jisem-journal.com/

Research Article



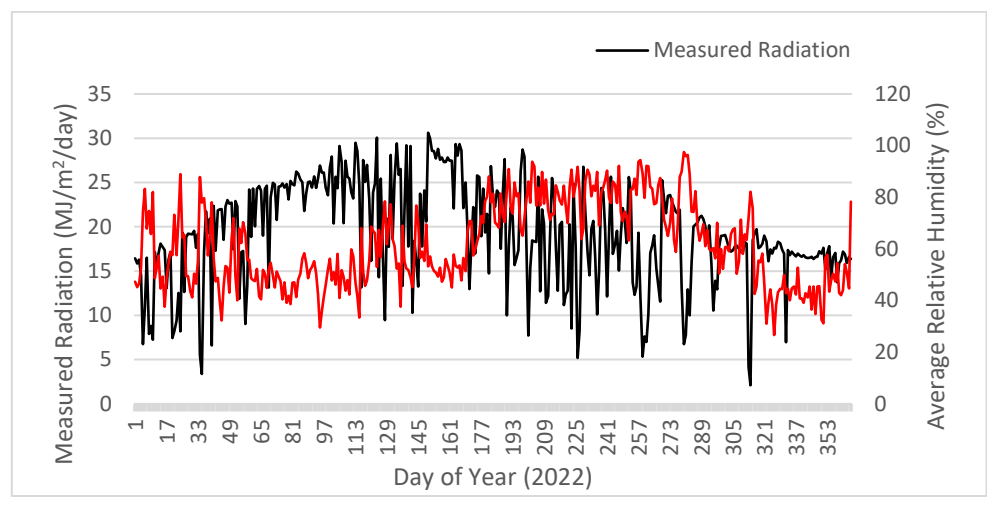


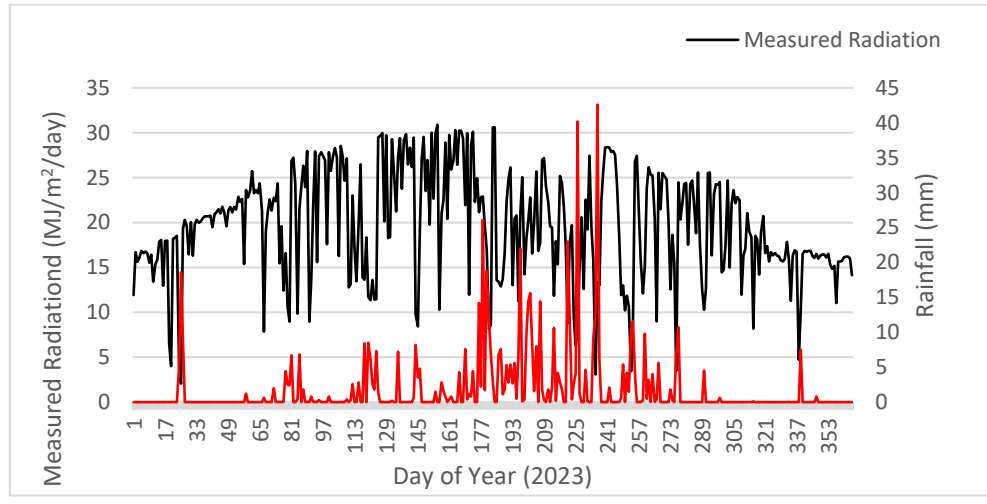


2025, 10(44s) e-ISSN: 2468-4376

https://www.jisem-journal.com/

Research Article





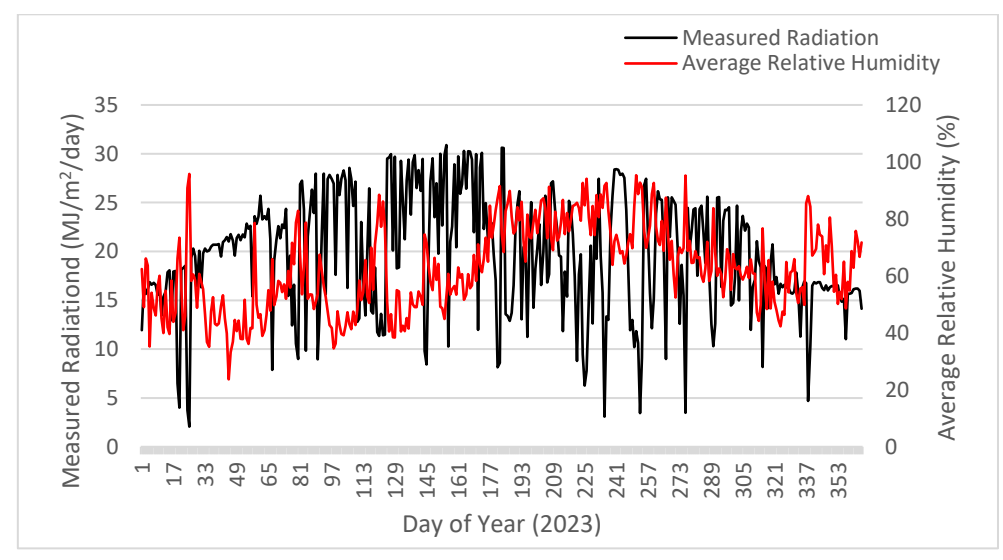


Fig. 9 Graphical Representations of Variation of Measured Solar Radiation with Temperature, Rainfall and Relative Humidity along the Day of Year 2022 and 2023 at Jumla, Nepal

CONCLUSIONS

2025, 10(44s) e-ISSN: 2468-4376

https://www.jisem-journal.com/

Research Article

The measured solar energy values were 18.9 MJ/m²/day in 2021, 19.3 MJ/m²/day in 2022, and 19.6 MJ/m²/day in 2023. The BC model emerged as the most effective among the four models tested. This was determined through error analysis, where in 2021, the RMSE was lower for the BC model compared to the DB and MDCBB models. Additionally, the MBE was smaller in the BC model than in the CD and DB models, and the R² value for the BC model was higher than all the other models. In 2022, the BC model again showed a lower RMSE compared to the CD and MDCBB models, a lower MBE than the CD and DB models, and a higher R² value than the other models. Similarly, in 2023, the BC model had a lower RMSE compared to the CD and MDCBB models, a smaller MBE than the DB model, and an R² value higher than that of the CD and MDCBB models, while matching the DB model.

From these results, it can be concluded that the BC model outperforms the other three. As a result, the BC model's coefficients can be applied to estimate solar energy at comparable locations in Nepal.

Acknowledgements:

The authors would like to sincerely thank the FAO SDRN Agrometeorology Group, Rome, Italy, and ISCI Crop Science, Bologna, Italy, for providing a free version of the RadEst ver. 3.00 software and manual through their website for academic use. They also express their gratitude to the Department of Hydrology and Meteorology, Government of Nepal, for supplying pyranometer data and other essential support.

REFERENCES

- [1] Acra, A., Raffoul, Z., & Karahagopian, Y. (1984). Solar disinfection of drinking water and oral rehydration solutions.
- [2] Bechini, L., Ducco, G., Donatelli, M., & Stein, A. (2000). Modelling, interpolation and stochastic simulation in space and time of global solar radiation. *Agriculture, Ecosystems & Environment*, 81(1), 29–42. https://doi.org/10.1016/S0167-8809(00)00170-5
- [3] Bristow, K. L., & Campbell, G. S. (1984). On the relationship between incoming solar radiation and daily maximum and minimum temperature. *Agricultural and Forest Meteorology*, 31(2), 159–166. https://doi.org/10.1016/0168-1923(84)90017-0
- [4] Chegaar, M., Lamri, A., Physique, A. C.-Rev. Energ. Ren.:, & 1998, undefined. (1998). Estimating global solar radiation using sunshine hours. *Researchgate.Net*, 7–11.
- [5] Donatelli, M., & Bellocchi, G. (2001a). Estimates of daily global solar radiation: New developments in the software RadEst3.00. In: Proceedings of International Symposium on modelling cropping System, 2nd edn, 16-18, 2001. Institute for CRN, Florence, Italy, pp 213-214.
- [6] Donatelli, M., & Bellocchi, G. (2001b). RADEST 3.00: software for the estimation of the solar global radiation. *Agrometeorologia.It*.
- [7] Donatelli, M., Bellocchi, G., & Fontana, F. (2003). RadEst3.00: Software to estimate daily radiation data from commonly available meteorological variables. *European Journal of Agronomy*, 18(3–4), 363–367. https://doi.org/10.1016/S1161-0301(02)00130-2
- [8] Donatelli, M., & Bellocchi, G. S. (1998) A simple model to estimate global solar radiation. In: Proceedings of the fifth congress of the European Society for Agronomy Nitrs, Slovakia, vol II, pp 133-134.
- [9] Government of Nepal. (2020). Economic Survey 2019/20. *Ministry of Finance*, 1–144. https://mof.gov.np/uploads/document/file/Economic Survey 2019_20201125024153.pdf
- [10] Iqbal, M. (1983). An introduction to solar radiation.
- [11] Joshi, U., Chapagain, N. P., Karki, I. B., Shrestha, P. M., & Poudyal, K. N. (2022). Estimation of daily solar radiation flux at Western Highland, Simikot, Nepal using RadEst 3.0 software. *International Journal of System Assurance Engineering and Management*, 13(1), 318–327. https://doi.org/10.1007/s13198-021-01234-4
- [12] Joshi, U., Shrestha, P. M., Maharjan, S., Maharjan, B., Chapagain, N. P., Karki, I. B., & Poudyal, K. N. (2021). Estimation of Solar Energy Using Different Empirical Models at Mid Hill, Nepal. *Journal of Nepal Physical Society*, 7(2), 42–48. https://doi.org/10.3126/JNPHYSSOC.V7I2.38621

2025, 10(44s) e-ISSN: 2468-4376

https://www.jisem-journal.com/

Research Article

- [13] Khatri Chhetri, B. R., & Gurung, S. (2017). Estimation of total solar radiation using RadEst 3.00 software at Jumla, Nepal. *International Journal of Systems Assurance Engineering and Management*, 8, 1527–1533. https://doi.org/10.1007/s13198-017-0625-5
- [14] Kipp, & Zonnen. (2006). CMP/CMA Series Instruction Manual, Kipp & Zonen B.V. Delftechpark 36, 2628 XH Delft, The Netherlands.
- [15] Pondyal, K., Bhattarai, B. K., Sapkota, B. K., & Kjeldstad, B. (2011). Solar radiation potential at four sites of Nepal. *Nepjol.Info*, 8(3), 189–197.
- [16] Poudyal, K. N. (2015). Estimation of Global Solar Radiation using Modifed Angstrom Empirical formula on the basis of Meterological parameters in Himalaya Region Pokhara, Nepal. *Journal of the Institute of Engineering*, 11(1), 158–164. https://doi.org/10.3126/jie.v11i1.14710
- [17] Poudyal, K. N., Bhattarai, B. K., Sapkota, B., & Kjeldstad, B. (2012). Estimation of the Daily Global Solar Radiation using RadEst 3.00 software-A Case Study at Low land Plain Region of Nepal. *Journal of Nepal Chemical Society*, 29, 48–57. https://doi.org/10.3126/jncs.v29i0.9237
- [18] Rajbanshi, B. K., Singh, R. G., KC, B. R., & Poudel, K. N. (2024). Comparative Analysis of Different Models within RadEst 3.0 for Solar Radiation Estimation at Dhankutta, Nepal. *Journal of Nepal Physical Society*, 10(1), 70–76. https://doi.org/10.3126/jnphyssoc.v10i1.72845
- [19] Rajbanshi, B. K., Singh, R. G., Khatiwada, K., & Thapa, A. (2024). Comparative Analysis of Empirical Models for Estimating Global Solar Radiation in Biratnagar, Nepal: A Case Study Using RadEst 3.0. In *Nanotechnology Perceptions ISSN* (Vol. 20, Issue S16). www.nano-ntp.com
- [20] Rajbanshi, B. K., Singh, R. G., Khatiwada, K., Thapa, A., Kharel, B., & Kc, B. R. (2025). Estimation of Global Solar Radiation in the Eastern Upland Region of Taplejung, Nepal, using RadEst 3.0 Software. In *Journal of Information Systems Engineering and Management* (Vol. 2025, Issue 16s). https://www.jisem-journal.com/
- [21] Schillings, C., Mannstein, H., & Meyer, R. (2004). Operational method for deriving high resolution direct normal irradiance from satellite data. *Solar Energy*, *76*, *475-484*.
- [22] Shrestha, J. R. (1998). "Experiences from Simikot Solar", Proceedings of International conference on Renewable Energy Technology for Rural Development (RETRUD-98), 12-14, October, Kathmandu, Nepal, 182-185.
- [23] Shrestha, J. N., Bajracharya, T. R, Shakya, S. R., & Giri, B. (2003). Renewable Energy in Nepal-Progress at a glance from 1998 to 2003. Proceeding of International conference on Renewable Energy Technology for Rural Development, 12-14, Kathmandu, Nepal, 1-11.
- [24] Shrestha, P. M., Karki, I. B., Chapagain, N. P., & Poudyal, K. N. (2019). Study of Linke Turbidity Factor on Solar Radiation over Jumla. *Molung Educational Frontier*, *9*, 141–149. https://doi.org/10.3126/MEF.V9I0.33595
- [25] WECS. (2023). Energy Synopsis Report, 2023.